Data Article

Relative sea-level data from the SEAMIS database compared to ICE-5G model predictions of glacial isostatic adjustment

Thomas Mann [a,*], Maren Bender [a,b], Thomas Lorscheid [a,b], Paolo Stocchi [c], Matteo Vacchi [d], Adam Switzer [e,f], Alessio Rovere [a,b]

[a] Leibniz Centre for Tropical Marine Research (ZMT), Fahrenheitstraße 6, 28359 Bremen, Germany
[b] University of Bremen, Center for Marine Environmental Sciences (MARUM), Leobener Straße 8, 28359 Bremen, Germany
[c] NIOZ Royal Netherlands Institute for Sea Research, Department of Coastal Systems, Utrecht University, Den Horn, Texel, the Netherlands
[d] Geography, College of Life and Environmental Sciences, University of Exeter, EX4 4RJ, Exeter, UK
[e] Asian School of the Environment, Nanyang Technological University, 649812, Singapore
[f] Earth Observatory of Singapore, Nanyang Technological University, 649812, Singapore

ARTICLE INFO

ABSTRACT

The SEAMIS database (Mendeley data repository; https://doi.org/10.17632/wp4ctb4667.1) contains 546 relative sea-level indicators from 31 different studies within the broader Southeast Asian region including the Maldives, India and Sri Lanka. Here we compare quality-controlled and site-specific relative sea-level data from 23 studies from the SEAMIS database to a suite of ICE-5G glacial isostatic adjustment models. The relation between robust and, if applicable, tectonically corrected relative sea-level data with the broad predictions of glacial isostatic adjustment models is interpreted and discussed in the article "Holocene sea levels in Southeast Asia, Maldives, India and Sri Lanka: The SEAMIS database" [1] in Quaternary Science Reviews.

Specifications Table

Subject area	Earth Sciences
More specific subject area	Coastal geomorphology
Type of data	Tables, graphs, figures, netCDF files
How data was acquired	Standardization of published data; modeling
Data format	Published RSL data: standardized and quality-controlled; netCDF files of modeled RSL: raw
Experimental factors	Data considered originate from previous studies carried out in Southeast Asia, Maldives, India and Sri Lanka and contain Holocene RSL information
Experimental features	Data were collected from literature review
Data source location	Southeast Asia, Maldives, India and Sri Lanka
Data accessibility	SEAMIS database and updates, netCDF files of ICE-5G model output and MATLAB script to plot data at https://github.com/Alerovere/SEAMIS; SEAMIS database containing RSL indicators also at https://doi.org/10.17632/wp4ctb4667.1

Value of the Data

- Data are useful to calibrate earth- and ice-models in glacial isostatic adjustment simulations
- Data is beneficial for modelers of glacial isostatic adjustment processes and field geologists in Southeast Asia
- Data can be easily updated by other researchers and compared to other models of glacial isostatic adjustment
- Data allow an evaluation of potential post-formational changes in the elevations of relative sea-level markers
- Data allow a validation of model parameters

1. Data

The dataset (i.e. the SEAMIS database as of July 2019) comprises 546 Holocene relative sea-level indicators for Southeast Asia and surrounding regions (https://github.com/Alerovere/SEAMIS, https://doi.org/10.17632/wp4ctb4667.1, [1]). Age-elevation information of published relative sea-

Table 1
Details on the Earth model parameters and different mantle viscosity profiles employed to simulate glacial isostatic adjustment in combination with the Ice model ICE-5G in the areas of interest. Model short names refer to the different model curves on Figs. 1–22.

| Model short name	Ice model	Earth model parameters
ice5g-vm2-90km.nc	ICE-5G	Upper Mantle = 0.25×10^{21} Pa•s Transition Zone = 0.5×10^{21} Pa•s Lower Mantle = 5×10^{21} Pa•s Lithosphere Thickness = 90 km
ice5g-vm2b-90km.nc	ICE-5G	Upper Mantle = 0.25×10^{21} Pa•s Transition Zone = 0.25×10^{21} Pa•s Lower Mantle = 5×10^{21} Pa•s Lithosphere Thickness = 90 km
ice5g-vm2-120km.nc	ICE-5G	Upper Mantle = 0.25×10^{21} Pa•s Transition Zone = 0.5×10^{21} Pa•s Lower Mantle = 5×10^{21} Pa•s Lithosphere Thickness = 120 km
ice5g-vm3-90km.nc	ICE-5G	Upper Mantle = 0.25×10^{21} Pa•s Transition Zone = 0.5×10^{21} Pa•s Lower Mantle = 10×10^{21} Pa•s Lithosphere Thickness = 90 km
ice5g-vm4-90km.nc	ICE-5G	Upper Mantle = 0.25×10^{21} Pa•s Transition Zone = 0.5×10^{21} Pa•s Lower Mantle = 100×10^{21} Pa•s Lithosphere Thickness = 90 km
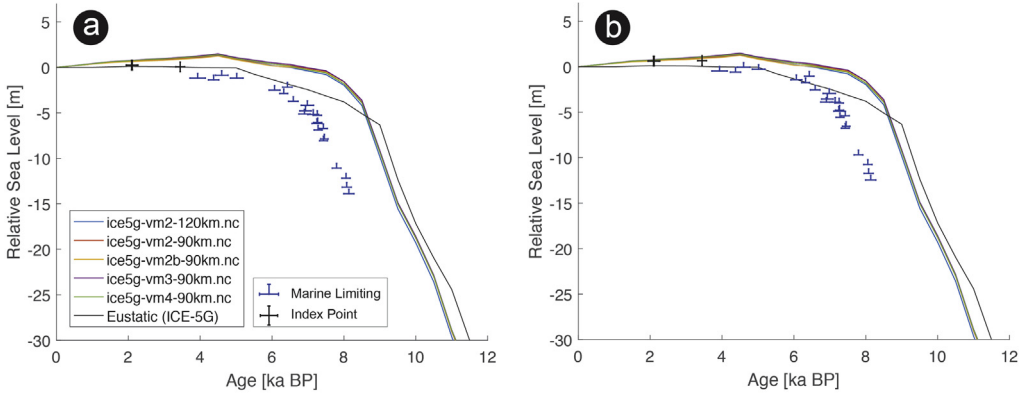
Fig. 1. Standardized Holocene relative sea-level data obtained from Ref. [4] in comparison to glacial isostatic adjustment geophysical model predictions for South Maalhosmadulu Atoll, Maldives. a) Original sample elevations are shown. b) Data corrected for subsidence based on a number of constraints regarding the timing and elevation of Last interglacial sea level and the magnitude of karstification resulting from subaerial exposure of the Last interglacial reef carbonate during the glacial (see Ref. [1] and above).
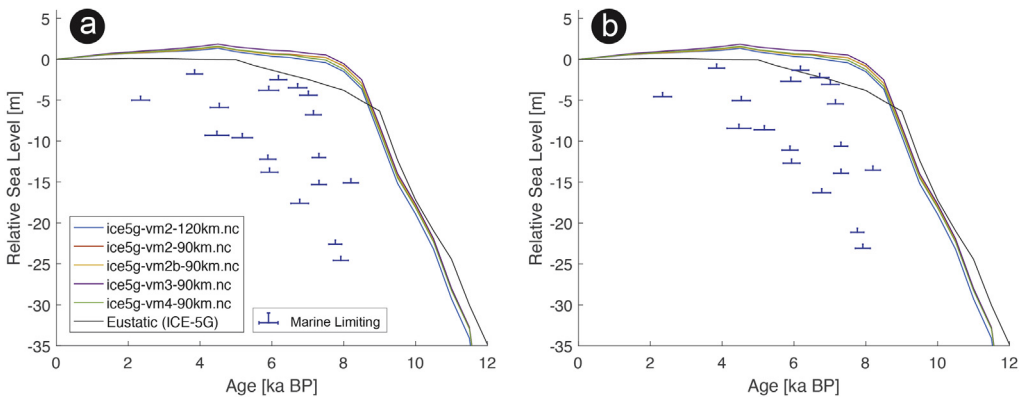
Fig. 2. Standardized Holocene relative sea-level data obtained from Ref. [5] in comparison to glacial isostatic adjustment geophysical model predictions for Palau Islands in the western Pacific. a) Original sample elevations are shown. b) Data corrected for subsidence based on a number of constraints regarding the timing and elevation of Last interglacial sea level and the magnitude of karstification resulting from subaerial exposure of the Last interglacial reef carbonate during the glacial (see Ref. [1] and above).

level data have been transformed into comparable relative sea-level indicators using a standardized protocol [2]. Quality-controlled, site-specific relative sea-level indicators are here compared to modeled relative sea-level change at each site generated with the ICE-5G geophysical model (Table 1, [3]).

The present dataset comprises a collection of RSL data from 23 studies that have been conducted in 22 locations. Figs. 1–22 present site-specific, standardized, quality-controlled and, if possible (see Ref. [1]), tectonically corrected age-elevation information of relative sea-level indicators together with the modeled relative sea level.
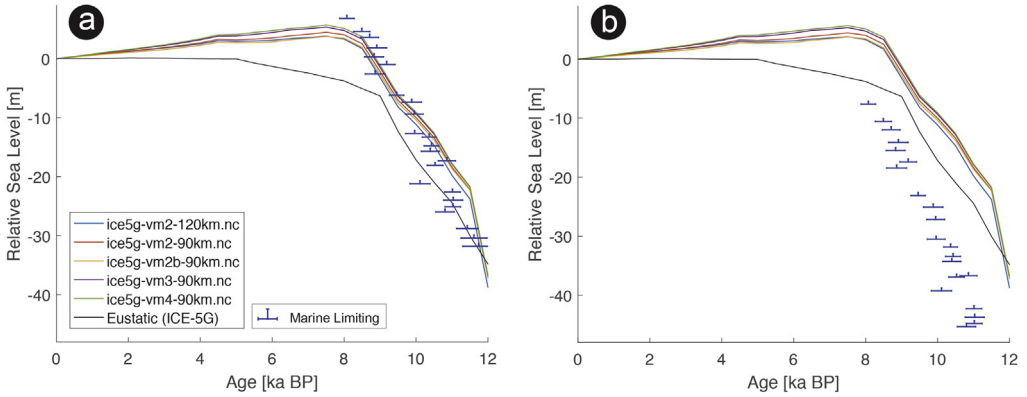
Fig. 3. Standardized Holocene relative sea-level data obtained from Ref. [6] in comparison to glacial isostatic adjustment geophysical model predictions for Huon Peninsula, Papua New Guinea. a) Original sample elevations are shown. b) Data corrected for tectonic uplift based on a number of constraints regarding the timing and elevation of Last interglacial sea level and the magnitude of karstification resulting from subaerial exposure of the Last interglacial reef carbonate during the glacial (see Ref. [1] and above).

2. Experimental design, materials and methods

2.1. Relative sea-level data

The methods that have been applied to compile a standardized dataset of sea-level index and limiting points meet the criteria recently summarized by Ref. [2]. In those sites where the elevation of the Pleistocene unconformity relative to the analyzed sequence of Holocene relative sea-level data is known [i.e., Refs. 4, 5, 6], the tectonic overprint resulting from active uplift or long-term subsidence has
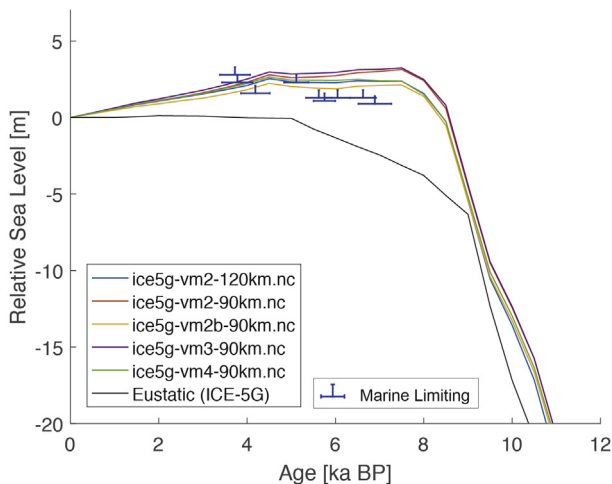

Fig. 4. Standardized Holocene relative sea-level data obtained from Ref. [7] in comparison to glacial isostatic adjustment geophysical model predictions for the section between Cape Comorin and Rameswaram in Southeastern India.
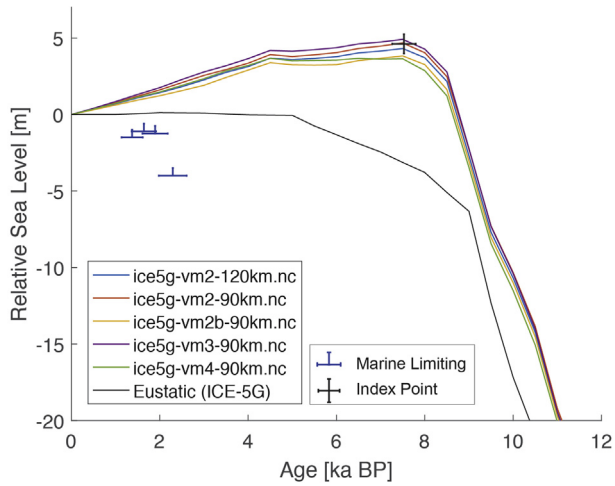
Fig. 5. Standardized Holocene relative sea-level data obtained from Ref. [8] in comparison to glacial isostatic adjustment geophysical model predictions for the Pulicat Lagoon in Southeastern India.
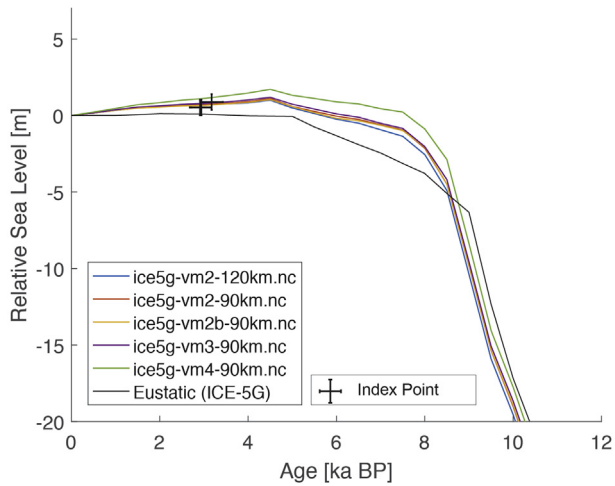

Fig. 6. Standardized Holocene relative sea-level data obtained from Ref. [9] in comparison to glacial isostatic adjustment geophysical model predictions for the Cocos (Keeling) Islands in the eastern Indian Ocean.
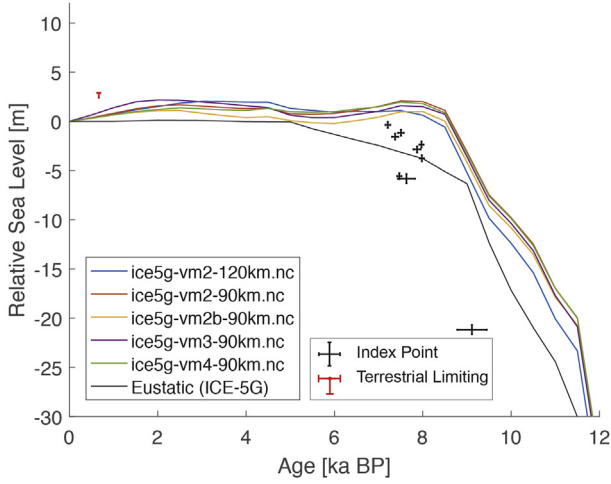
Fig. 7. Standardized Holocene relative sea-level data obtained from Ref. [10] in comparison to glacial isostatic adjustment geophysical model predictions for the Mekong River lowland near Phnom Penh, Cambodia.
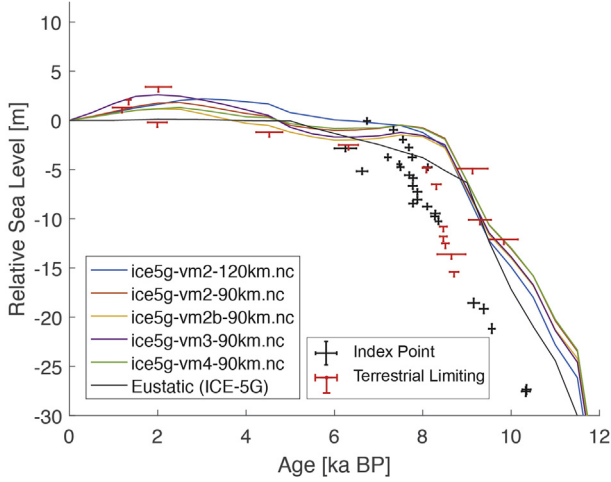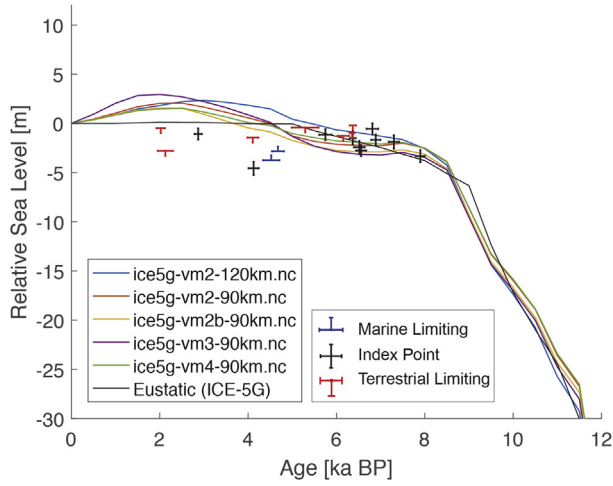

Fig. 8. Standardized Holocene relative sea-level data obtained from Ref. [11] in comparison to glacial isostatic adjustment geophysical model predictions for the Mekong River lowland near Phnom Penh, Cambodia.

Fig. 9. Standardized Holocene relative sea-level data obtained from Ref. [12] in comparison to glacial isostatic adjustment geophysical model predictions for the northeastern Mekong River Delta, Vietnam.
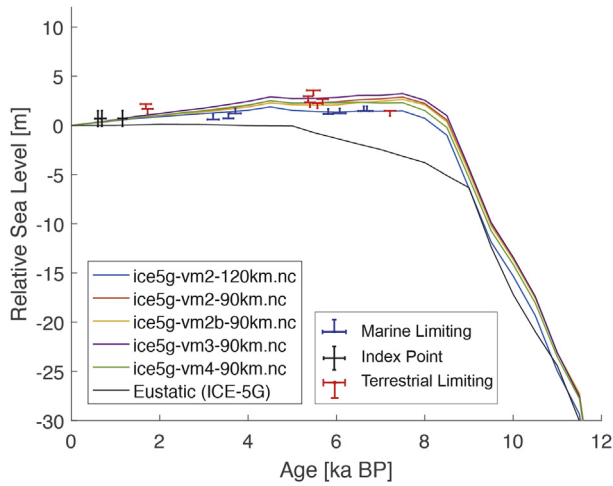

Fig. 10. Standardized Holocene relative sea-level data obtained from Ref. [13] in comparison to glacial isostatic adjustment geophysical model predictions for the section between Cà Ná and Son Hài in southeast Vietnam.
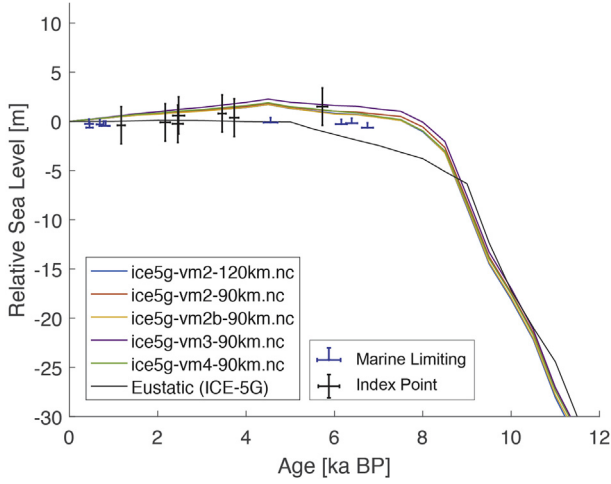
Fig. 11. Standardized Holocene relative sea-level data obtained from Ref. [14] in comparison to glacial isostatic adjustment geophysical model predictions for the Phang-nga Province, Thailand.
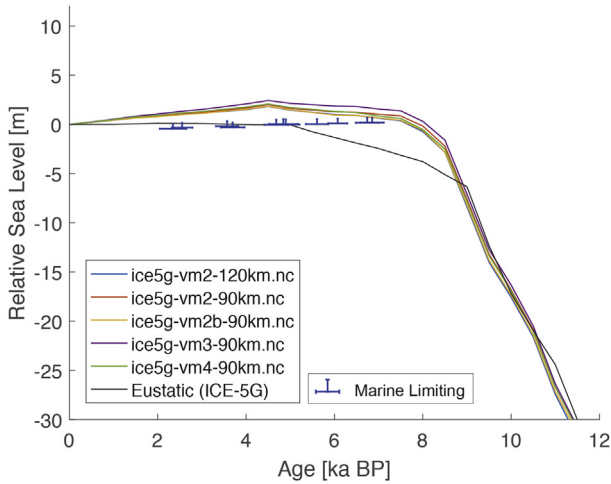

Fig. 12. Standardized Holocene relative sea-level data obtained from Ref. [15] in comparison to glacial isostatic adjustment geophysical model predictions for Phuket, South Thailand.
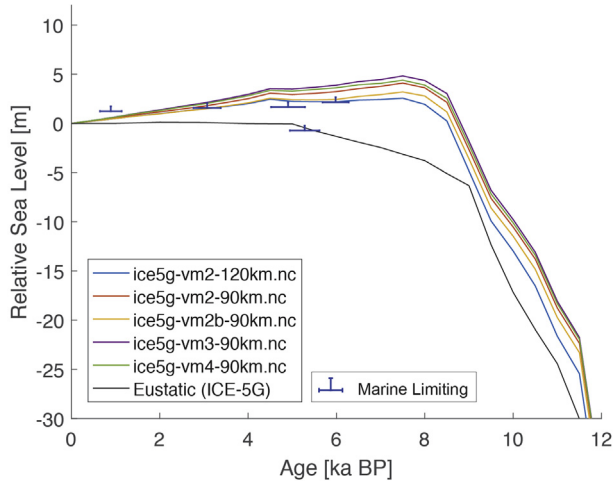
Fig. 13. Standardized Holocene relative sea-level data obtained from Ref. [16] in comparison to glacial isostatic adjustment geophysical model predictions for the section between Langkawi and Terengganu-Pahang at the west coast of Peninsular Malaysia.
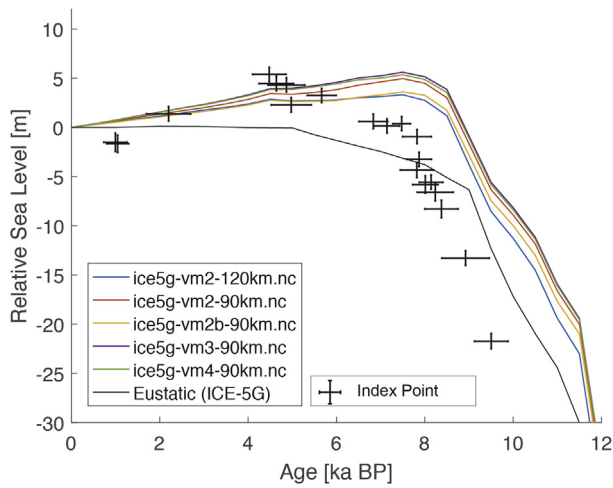

Fig. 14. Standardized Holocene relative sea-level data obtained from Ref. [17] in comparison to glacial isostatic adjustment geophysical model predictions for the section between Port Dickinson, Malaysia and Singapore.
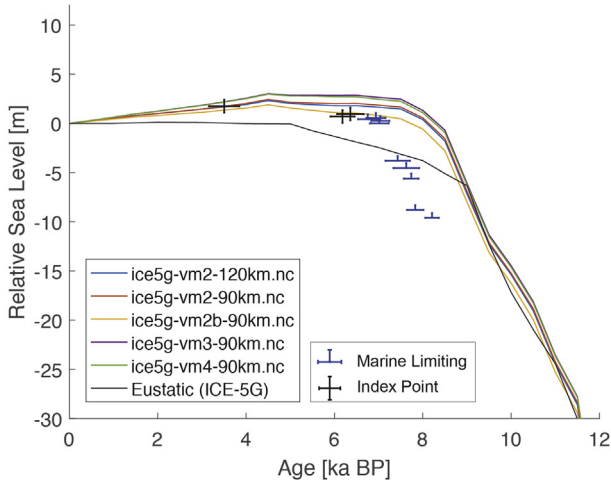
Fig. 15. Standardized Holocene relative sea-level data obtained from Ref. [18] in comparison to glacial isostatic adjustment geophysical model predictions for the Sungei Nipah catchment, Singapore.
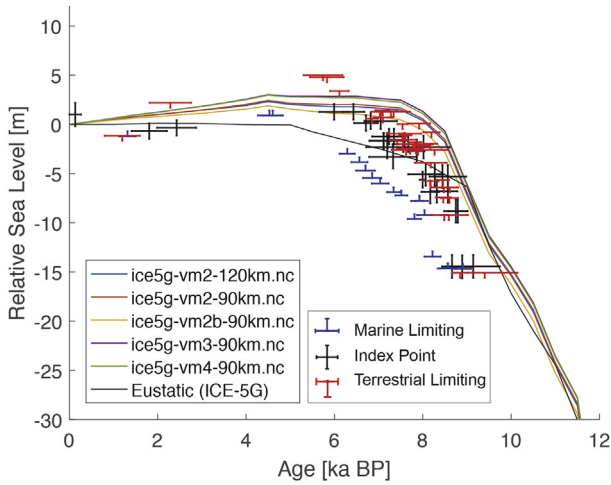

Fig. 16. Standardized Holocene relative sea-level data obtained from Refs. [19,20] in comparison to glacial isostatic adjustment geophysical model predictions for the Geylang district, Singapore.
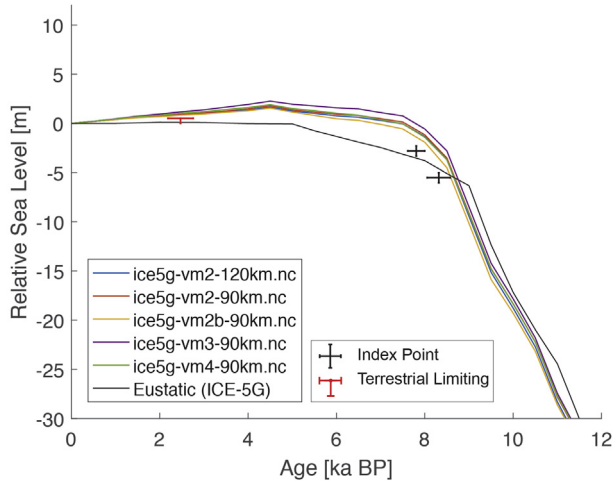
Fig. 17. Standardized Holocene relative sea-level data obtained from Ref. [21] in comparison to glacial isostatic adjustment geophysical model predictions for the Great Songkhla Lakes, Malay-Thai Peninsula.
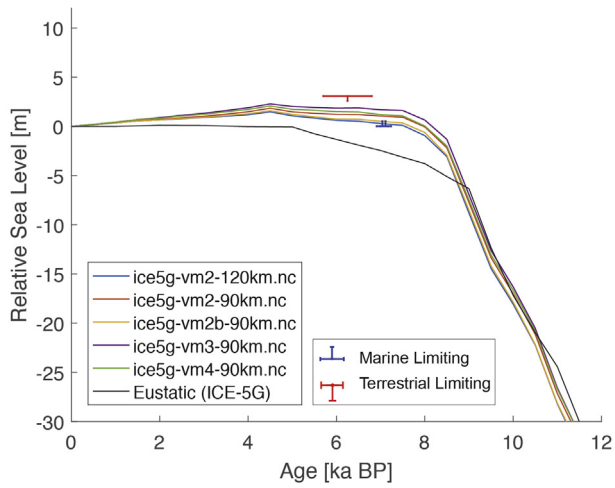

Fig. 18. Standardized Holocene relative sea-level data obtained from Ref. [22] in comparison to glacial isostatic adjustment geophysical model predictions for the area near Merang, Malaysia.

Fig. 19. Standardized Holocene relative sea-level data obtained from Ref. [23] in comparison to glacial isostatic adjustment geophysical model predictions for Kelang and Kuantan, Peninsular Malaysia.

Fig. 20. Standardized Holocene relative sea-level data obtained from Ref. [24] in comparison to glacial isostatic adjustment geophysical model predictions for Tioman Island, Malaysia.

Fig. 21. Standardized Holocene relative sea-level data obtained from Ref. [25] in comparison to glacial isostatic adjustment geophysical model predictions for the Belitung area, Indonesia.
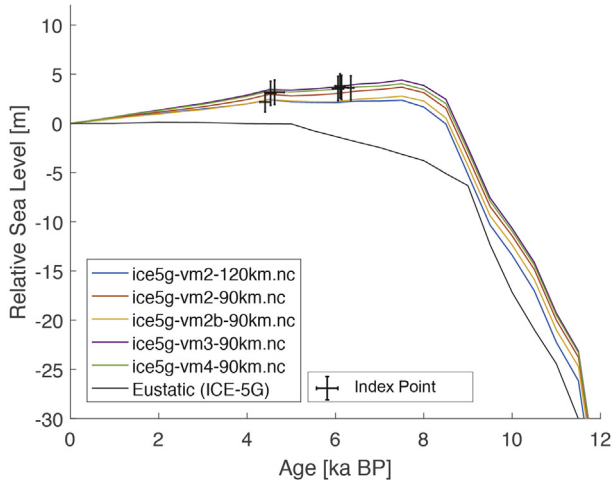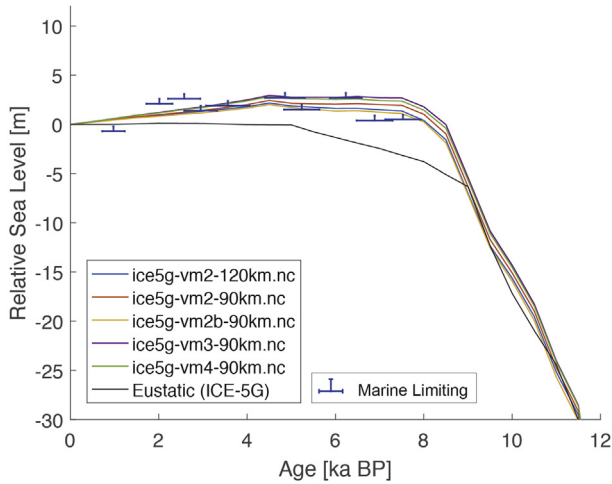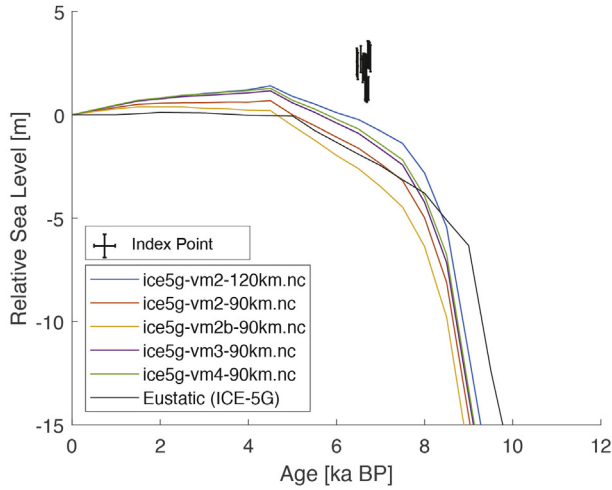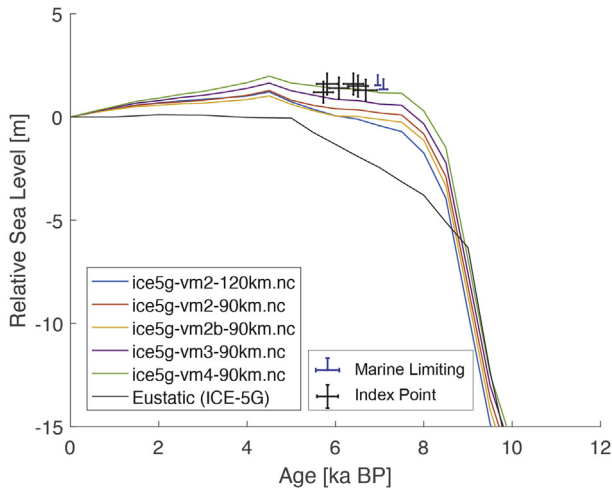

Fig. 22. Standardized Holocene relative sea-level data obtained from Ref. [26] in comparison to glacial isostatic adjustment geophysical model predictions for Teluk Awur, Indonesia.

been calculated. First, the average uplift/subsidence rate U has been calculated at each site. In doing so, minimum and maximum rates have been determined by dividing the minimum/maximum vertical displacements (based on the actual position of the Pleistocene Reef and a Last Interglacial sea level between 6 and 9 m above present) by the minimum/maximum time elapsed (based on a Last Interglacial between 116 ka BP and 129 ka BP). The average rate U is the sum of the minimum and maximum rates divided by 2 (negative rate for uplift, positive rate for subsidence). Calculated rates U

are 0.18 m/ka for South Maalhosmadulu Atoll, Maldives [4], 0.19 m/ka for Palau Islands in the western Pacific [5] and −1.79 m/ka for Huon Peninsula, Papua New Guinea [6]. The corrected relative sea-level position at each site is then calculated as H + U × tc [following Ref. 6] where H is the actual sample elevation and tc the radiocarbon age of the sample. Details on the reconstructions of site-specific relative sea-level positions can be found in Ref. [1].

2.2. Glacial isostatic adjustment models

To compute the contribution of glacial isostatic adjustment to relative sea-level changes, we have solved the Sea Level Equation [27,28] by means of the SELEN program [29]. We employed a 1-D, radially stratified, self-gravitating, rotating, Maxwell viscoelastic and incompressible Earth model and the ice-sheet model ICE-5G [3]. To explore the sensitivity of the predictions to various aspects of the model, we employed different mantle viscosity profiles and lithosphere thicknesses (Table 1). All model runs include time varying coastline positions [3,30].

Acknowledgements

Conflict of Interest

The authors declare that they have no known competing financial interests or personal relationships that could have appeared to influence the work reported in this paper.

References

[1] T. Mann, M. Bender, T. Lorscheid, P. Stocchi, M. Vacchi, A. Switzer, A. Rovere, Holocene sea levels in Southeast Asia, Maldives, India and Sri Lanka: the SEAMIS database, Quat. Sci. Rev. 219 (2019) 112−125.

[2] I. Shennan, A.J. Long, B.P. Horton, Handbook of Sea-Level Research, John Wiley & Sons, 2015.

[3] W.R. Peltier, Global glacial isostasy and the surface of the ice-age Earth: the ICE-5G (VM2) model and GRACE, Annu. Rev. Earth Planet Sci. 32 (2004) 111−149.

[4] P.S. Kench, S.G. Smithers, R.F. Mclean, S.L. Nichol, Holocene reef growth in the Maldives: evidence of a mid-Holocene sea-level highstand in the central Indian Ocean, Geology 37 (2009) 455−458, https://doi.org/10.1130/G25590A.1.

[5] H. Kayanne, H. Yamano, R.H. Randall, Holocene sea-level changes and barrier reef formation on an oceanic island, Palau Islands, western Pacific, Sediment. Geol. 150 (2002) 47−60, https://doi.org/10.1016/S0037-0738(01)00267-6.

[6] J. Chappell, H. Polach, Post-glacial sea-level rise from a coral record at Huon Peninsula, Papua New Guinea, Nature 349 (1991) 147−149, https://doi.org/10.1038/349147a0.

[7] P.K. Banerjee, Holocene and Late Pleistocene relative sea level fluctuations along the east coast of India, Mar. Geol. 167 (2000) 243−260.

[8] G.G. Vaz, P.K. Banerjee, Middle and late Holocene sea level changes in and around Pulicat Lagoon , Bay of Bengal , India, Mar. Geol. 138 (1997) 261−271.

[9] C. Woodroffe, R. McLean, H. Polach, E. Wallensky, Sea level and coral atolls: late Holocene emergence in the Indian Ocean, Geology 18 (1990) 62−66.

[10] T. Tamura, Y. Saito, S. Sieng, B. Ben, M. Kong, Depositional facies and radiocarbon ages of a drill core from the Mekong River lowland near Phnom Penh, Cambodia: evidence for tidal sedimentation at the time of Holocene maximum flooding 29 (2007) 585−592, https://doi.org/10.1016/j.jseaes.2006.03.009.

[11] T. Tamura, Y. Saito, S. Sieng, B. Ben, M. Kong, I. Sim, S. Choup, F. Akiba, Initiation of the Mekong River delta at 8 ka: evidence from the sedimentary succession in the Cambodian lowland, Quat. Sci. Rev. 28 (2009) 327−344, https://doi.org/10.1016/j.quascirev.2008.10.010.

[12] T.J.J. Hanebuth, U. Proske, Y. Saito, V.L. Nguyen, T.K.O. Ta, Early growth stage of a large delta—transformation from estuarine-platform to deltaic-progradational conditions (the northeastern Mekong River Delta, Vietnam), Sediment. Geol. 261 (2012) 108−119.

[13] K. Stattegger, R. Tjallingii, Y. Saito, M. Michelli, N. Trung Thanh, A. Wetzel, Mid to late Holocene sea-level reconstruction of Southeast Vietnam using beachrock and beach-ridge deposits, Glob. Planet. Chang. 110 (2013) 214–222, https://doi.org/10.1016/j.gloplacha.2013.08.014.

[14] A. Scheffers, D. Brill, D. Kelletat, H. Bruckner, S. Scheffers, K. Fox, Holocene sea levels along the Andaman Sea coast of Thailand, Holocene 22 (2012) 1169–1180, https://doi.org/10.1177/0959683612441803.

[15] T.P. Scoffin, M.D.A. Le Tissier, Late Holocene sea level and reef-flat progradation, Phuket, South Thailand, Coral Reefs 17 (1998) 273–276, https://doi.org/10.1007/s003380050128.

[16] H.D. Tjia, S. Fujii, Late quaternary shorelines in Peninsular Malaysia, Coast. Zo. Penins. Malaysia 2 (1992) 28–41.

[17] M.A. Geyh, H.-R. Kudrass, H. Streif, Sea-level changes during the late Pleistocene and Holocene in the Strait of Malacca, Nature (1979), https://doi.org/10.1038/278441a0.

[18] P.A. Hesp, C.C. Hung, M. Hilton, C.L. Ming, I.M. Turner, A first tentative Holocene sea-level curve for Singapore, J. Coast. Res. 14 (1998) 308–314.

[19] M.I. Bird, L.K. Fifield, T.S. Teh, C.H. Chang, N. Shirlaw, K. Lambeck, An inflection in the rate of early mid-Holocene eustatic sea-level rise: a new sea-level curve from Singapore, Estuar. Coast Shelf Sci. 71 (2007) 523–536, https://doi.org/10.1016/j.ecss.2006.07.004.

[20] M.I. Bird, W.E.N. Austin, C.M. Wurster, L.K. Fifield, M. Mojtahid, C. Sargeant, Punctuated eustatic sea-level rise in the early mid-Holocene, Geology 38 (2010) 803–806, https://doi.org/10.1130/G31066.1.

[21] B.P. Horton, P.L. Gibbard, G.M. Mine, R.J. Morley, C. Purintavaragul, J.M. Stargardt, Holocene sea levels and palaeoenvironments, Malay-Thai Peninsula, southeast Asia, Holocene 8 (2005) 1199–1213.

[22] P.R. Parham, Y. Saito, N. Sapon, R. Suriadi, N.A. Mohtar, Evidence for ca. 7-ka maximum Holocene transgression on the Peninsular Malaysia east coast, J. Quat. Sci. 29 (2014) 414–422, https://doi.org/10.1002/jqs.2714.

[23] H. Kamaludin, Holocene Sea Level Changes in Kelang and Kuantan, Peninsular Malaysia, Ph. D. thesis, 2001, p. 309.

[24] H.D. Tjia, S. Fujii, K. Kigoshi, Holocene shorelines of Tioman island in the South China sea, in: J.H.J. Terwindt, H. Van Steijn (Eds.), Developments in Physical Geogrqphy - a Tribute to J. I. S. Zonneveld. Geologie en Mijnbouw, 1983, pp. 599–604.

[25] A.J. Meltzner, A.D. Switzer, B.P. Horton, E. Ashe, Q. Qiu, D.F. Hill, S.L. Bradley, R.E. Kopp, E.M. Hill, J.M. Majewski, D.H. Natawidjaja, B.W. Suwargadi, Half-metre sea-level fluctuations on centennial timescales from mid-Holocene corals of Southeast Asia, Nat. Commun. 8 (2017) 14387, https://doi.org/10.1038/ncomms14387.

[26] K. Azmy, E. Edinger, J. Lundberg, W. Diegor, Sea level and paleotemperature records from a mid-Holocene reef on the North coast of Java, Indonesia, Int. J. Earth Sci. 99 (2010) 231–244, https://doi.org/10.1007/s00531-008-0383-3.

[27] W.E. Farrell, J.A. Clark, On postglacial sea level, Geophys. J. Int. 46 (1976) 647–667.

[28] J.X. Mitrovica, W.R. Peltier, On postglacial geoid subsidence over the equatorial oceans, J. Geophys. Res. 96 (1991) 20053–20071.

[29] G. Spada, P. Stocchi, SELEN: a Fortran 90 program for solving the "sea-level equation", Comput. Geosci. 33 (4) (2007) 538–562.

[30] W.R. Peltier, Ice age paleotopography, Science 265 (5169) (1994) 195–201.